Numerical Analysis of Solar Collector Absorber Tubes with C-shaped Roughness for Enhanced Heat Transfer

Abhishek Agarwal [1*]

[1]Department of Mechanical Engineering, College of Science & Technology, Royal University of Bhutan, 21101 Phuentsholing, Bhutan

Abstract. Solar collector absorber tubes perform a significant function in solar power devices that concentrate the solar energy into a single cylindrical absorber tube. Characteristically, this type of tube is covered with a smooth surface. The purpose of this study is to simulate the convectional behaviour of these absorber tubes with the help of numerical calculation methods like Computational Fluid Dynamics (CFD). The collector tube CAD model has been made using the Creo design software and the ANSYS CFX software is used for the CFD simulations corresponding to the three mass_flow rates (0.005Kg/s, 0.010Kg/s, and 0.015Kg/s). The heat transfer is improved by tweaking the absorber tube with a C-shaped corrugated roughness profile. The choice of the Shear Stress Transport turbulence (SSTT) model for analysis is justified by its capability to accurately predict both laminar and turbulent flows, which is why it is considered to be suitable for the absorber tube with a cross-sectional shape. Findings demonstrated that the use of C-shaped artificial roughness led to a substantial rise in convective heat transfer, for 6.016% of the thermal conductivity was taken into account. The SST turbulence model verifies its efficacy by predicting the fluid flow patterns across the absorber tubes. This study forms the basis for developing new mechanical efficiency metrics for solar collector absorber tubes, which is significant for solar energy technology development.

1 Introduction

Being the core of development and progress, the energy makes its way through all the discipline sectors while at the same time improving the quality of life globally. Our planet is very rich in regards to the kinds of energy resources that it possesses, ranging from traditional sources like coal and oil to renewable resources that include solar, wind, and hydroelectric power [1]. Nevertheless, the functional use of conventional resources has intensely provoked their rapid extraction which encourages the investigation of sustainable and alternative sources of energy for long-term use. The sustainability issue has been answered by renewable energy, which is a viable and durable alternative, and therefore meets global electric demands while minimizing dependency on exhaustible fossil fuels. Out of the renewables, solar energy can be said to have its own promotion due to its abundance, cleanliness, and non-emission of greenhouse gases [2]. The enormous capacity of solar power is unfortunately not at all exploited at the very least as only a small part of this power is harnessed being used for electricity generation at the worldwide level. Nevertheless, the enhancements in technology and the heightened awareness of the advantages of this energy source are the cause of the shift towards a considerable acceptance of solar energy solutions.

The parabolic trough solar collector (PTSC or PTC) is known to be one of the vibrant technologies in the sector of solar energy applications [3]. PTSC is a kind of CSP system that uses curved, reflective surfaces to collect sunlight and focus it into a small area where the resulting heat can be turned into useful energy [4]. While this heat is generated, it is used to create steam, which in turn activates a turbine to generate electricity. As shown in Figure 1, PTSCs are known for their high efficiency and reliability, therefore, it is often used for large-scale solar power plants that are spread all over the world.

Fig. 1. Parabolic trough collector [5]

Through the practice of conventional flat-plate collectors, early systems were able to provide hot water temperatures up to 100 °C whereas modern closed-loop solar systems have preferably started using the new technology of parabolic dish collectors for low-to-medium temperature applications. This transition is an

* Corresponding author: agarwala.cst@rub.edu.bt

outcome of their high heat retention capability which influences the efficiency of the system thermally and also the functioning of the thermodynamics system. The present study intends to carry out a numerical analysis of the features of a PTC. The research concentrates on determining technical factors linked to heat retention, thermal efficiency, and thermodynamic performance, in particular. Through such a numerical illustration, this research tries to present the operating requirements of PTSC technology and its real potential for practical application.

The literature review as an excellent resource brings in some informative findings on research, development, and use of the PTC technology. K. Ravi Kumar et. al [6] employed the RNG K- turbulent model to numerically analyze a disk receiver, which is made porous, in a parabolic trough collector (PTC) for calculations with Therminol-VP1 as a working fluid. The research demonstrated that the disk distance (w) greatly affects the Nusselt_number and the drag force, with a 64.3% increase in heat_transfer performance achieved using a disk configuration (H=0.5) contrasted to cylindrical libraries.

In the other work, D.K.S. Reddy et al. [7] performed a numerical analysis on a solar PTC, which was subjected to varying thickness, porosity, and fin aspect ratio under different heat flux conditions. Besides, they proposed an optimized scheme of PTC with porous topography, emphasizing the relevance of fin receiver configuration and longitudinal fin in terms of efficiency.

K.S. Reddy et al. [8] executed a numerical study by using ANSYS FLUENT for a collector constructed of a stainless-steel tube with square, triangular, and trapezoidal inserts. According to the study, there was a satisfying agreement between solutions obtained from CFD and Dittus-Boulter's equation, with an error of only 4.7%. Heat transfer enhancement went from 2% to 8%.

H.P. Wang, C. Xu, and D.Y. Liu [9] performed a specific numerical analysis on PTC, which studied the thermo-hydraulic performance of different metal foams with different porosities and geometrical characteristics. The statistical data showed a fall in the maximum circumferential temperature difference to 45% level which eliminated thermal stress. Salazar et.al. [10] introduce parabolic trough solar collectors as a progressive science, which the authors analyze in terms of thermal performance, collector components, applications, and construction materials. The study covers solar light conversion experiences, the latest technologies, efficiency analysis with software, international standards, and market scenarios, aiming to have further development of this technology. Siraj et.al. [11] conducted the performance-evaluation of a PTSC with the thermal-storage tank of quadrilateral box shapes storing Stearic_acid 0.3vol% as nanofluids of Phase-change Material (PCM). They varied the flow rates of the oil waste and water (0.035, 0.045, and 0.065 kg/sec) to determine the heat output of collectors' receivers and the storage tank's efficacy. The research observed that at an airstream of 0.035 kg/sec the collector with the storage tank produced a heat gain of 10441 W for water and 13724W for used engine oil, the heat gain for the second one being 0.31 times greater than that for water.

The case study confirms that waste engine oil takes heat faster than water when both are at the same flow rate. Mohamed et al. [12] focused on the possibilities of electricity generation through an ORC system using the waste heat of cement in an industrial process. The proposed approach called for a hybrid energy system that blends heat recovery (WHR) from the industrial furnaces' flue gases using a Parabolic-Trough Solar Collector (PTSC) with solar energy. The heat medium-grade ORC system was designed to use temperature alternation starting from 250 °C to 380 °C for electricity production. The functionality of each component was underscored and improved, indisputably illustrating that the ORC was capable of delivering a maximum output power of 323- 360 kW, in less than 3.75 years for an investment payback period and was saving net $280,000 per year. The research shows that some of the main reasons for using ORC to generate power in HWP and other industrial settings are economic and environmental.

These studies [13], [14], [15], [16], [17] at large collectively show that the PTSC technology is quite advanced and a promising alternative for ensuring a steady energy supply in a sustainable and efficient manner. While the solar collector technology improvements have been considerable, there is a considerable lack of comprehensive research conducting precise analysis of the absorbance tube surface structures. The performance of collectors has been investigated extensively in some studies but only considering the whole system and neglecting the specifics of absorber tube design and its role in heat transfer. This research is designed to fill the gap represented by the evaluation of thermal conductivity in C-shape roughness tubes. It will provide researchers with an opportunity to acquire a solid knowledge of the efficiency of heat_transfer within solar water heaters. The thermal efficiency of solar collector tubes is a key factor determining the system efficiency of solar energy technologies. Although it is difficult to obtain such thorough studies of the effect that specific roughness profiles have on tube efficiency. It has been hypothesized that the introduction of a C-shape patterned roughness profile on the tube absorbers will enhance the Heat_transfer rate and this will compare to that of smooth tubes at a better degree.

The roughness profile is anticipated to contribute to increased local turbulence and heat exchange in the fluid, and a peak performance of the solar collector system will be achieved as a result.

Therefore, we consider the following research questions-

1. Is there a systematic method for the introduction of uniform roughness C-shaped absorber tubes that can be compared to the smooth tube performance?
2. How is the heat_transfer augmentation in absorber tubes with C-shape artificial roughness affected by the changes in mass_flow rates?

3. What will be the convective heat transfer rate when C-shaped artificial roughness is added beside the absorber tubes which are without roughness?

This study is concerned with the application of the available CFD methods to investigate the local behavior of an absorber tube exposed to direct irradiance from a solar collector by conducting the necessary calculations. A CAD model of the collector tube is created using Creo design software, and CFD simulations are performed in ANSYS CFX for varying mass_flow rates: Hence, the mass_flow rates are 0.005 kg/s, 0.010 kg/s, and 0.015 kg/s respectively. Therefore, to achieve high Heat_transfer performance, the absorber tube has been given a rough profile of a C-shape. The analysis actively utilizes, the Shear Stress Transport turbulence (SSTT) model.

2 Methodology

The absorber tube is modelled with varying depths of C-shape roughness profiles (5mm, 7mm, and 9mm) using 3D parametric Creo modelling software. The tube's model is developed using revolve and cut tools based on reference dimensions from literature. The absorber tube has a length of 1.20m, an inside diameter of 0.027m, and an outside diameter as per [18]. Figure 2 shows a CAD Model of a PTC with a roughness of depth of 5mm and a C-shape and Figure 3 depicts the enlarged view roughness of depth 5mm respectively.

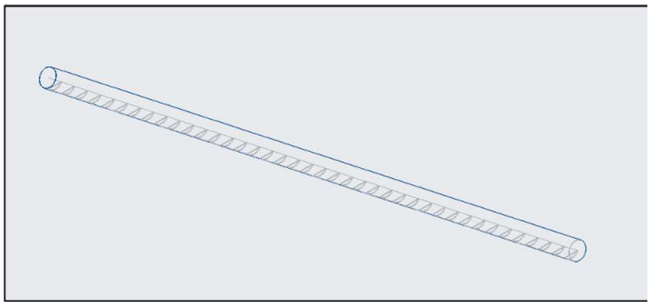

Fig. 2. PTC CAD Model with roughness of depth 5mm and C-shape

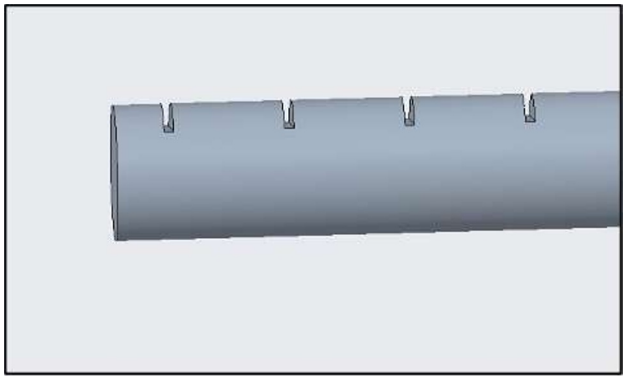

Fig. 3. Enlarged view roughness of depth 5mm

2.1 Conversion of CAD Model and Meshing

The CAD model is transformed into the iges format for export to the ANSYS_modeler. This conversion is done to identify geometric errors such as hard angles and edges. The model is meshed using tetrahedral components with an element sizing of 1.5mm due to their suitability for complex geometries and irregular shapes [19]. The relevance center is set to medium, the span angle center to fine, and the smoothing to medium.

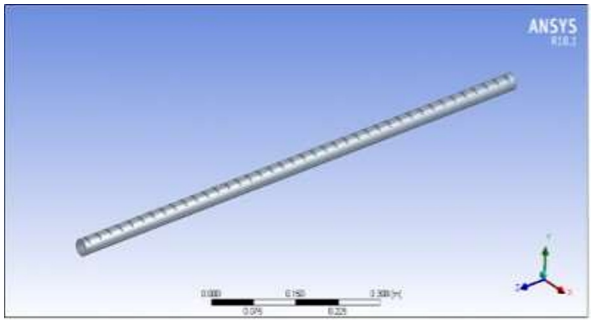

Fig. 4. Imported CAD model in ANSYS design modeler

This results in 55961 nodes and 181668 elements. The CAD model in the ANSYS_design modeler is shown in Figure 4 while the meshed CAD model in ANSYS is displayed in Figure 5.

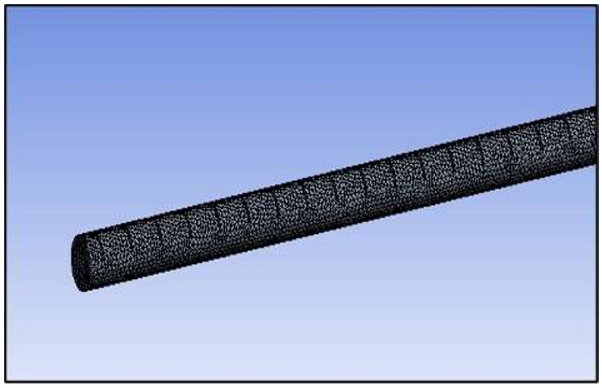

Fig. 5. Meshing CAD model in ANSYS

2.2 Fluid Domain and Boundary Conditions

The domain is characterized as a fluid with isothermal-energy conditions and a pressure of one atm. The SSTT model is selected for the investigation due to its efficiency in simpler liquid flow predictions. The analysis is conducted for three mass_flow rates (0.005Kg/s, 0.010Kg/s, and 0.015Kg/s) and three roughness depths. A heat flux of 744W/m2 is applied to the absorber tube wall. Inlet boundary conditions are well-defined with a water inlet, while outlet boundary conditions include a relative pressure of 0Pa as shown in Figures 6 and 7 respectively.

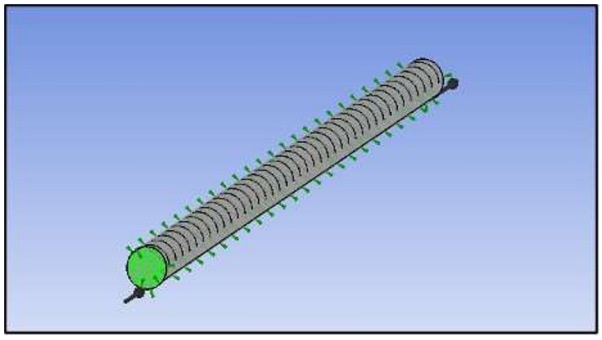

Fig. 6. Defined Water-inlet boundary condition

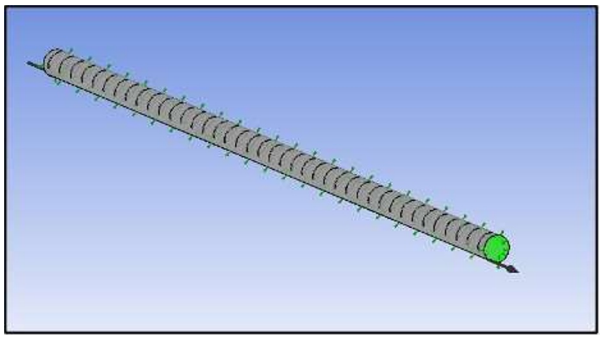

Fig. 7. Defined Water-outlet boundary condition

2.3 Simulation and Convergence

RMS residual target values are set to 0.00001, the advection scheme to double precision, and the turbulence numeric to 1st order. The simulation is run until convergence is achieved. Compared to other models, the Shear-Stress Transport (SSTT) turbulence model was chosen because it is capable of predicting both laminar and turbulent flows very well – making it applicable to a variety of flow situations [20], [21]. This model lays upon the successful qualities of k-ε and k-ω models, inclusively used in the flow with boundary layer separation and reattachment. Furthermore, its computational efficiency helps to solve complex geometrical simulations and large systems of equations similar to the absorber tube with a cross-shaped roughness in this study. It is thus the strategy that makes it possible to have a comprehensive study on the temperature characteristics of absorber tubes containing C-shape roughness profiles and hence addresses the topics of Heat_transfer efficiency of solar collector systems.

3 Results and discussion

The CFD analysis considered the thermal effects of the C-shaped roughness inside of absorber tubes with depth values of 5mm, 7mm, and, 9mm. The analysis goal was to uncover the pressure drop, temperature distribution, and Heat_transfer coefficient. Additionally, a comparative analysis of Reynolds number and Nusselt_number was conducted for three diverse mass_flow rates (0.005Kg/s, 0.010Kg/s, and 0.015Kg/s).

3.1 Parameters for absorber tube without roughness and C-shape (Traditional)

The temperature plots showed an increase in temperature from the inlet to the outlet of the absorber tube, with values close to literature references. Figure 8 represents a temperature distribution plot across the lateral plane.

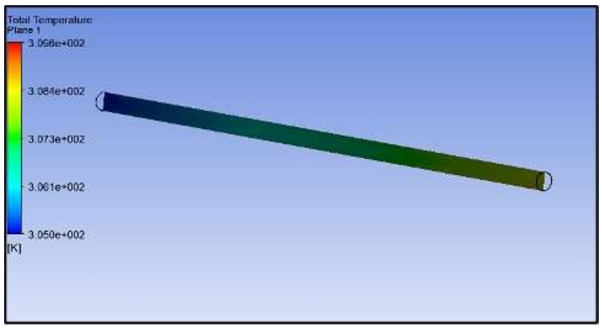

Fig. 8. Temperature plot at .005kg/s

The temperature plot shows a low inlet temperature, increasing towards the outlet of the absorber tube. The temperature near the inlet is 305K, increasing to 308K towards the exit, in close agreement with the literature [18].

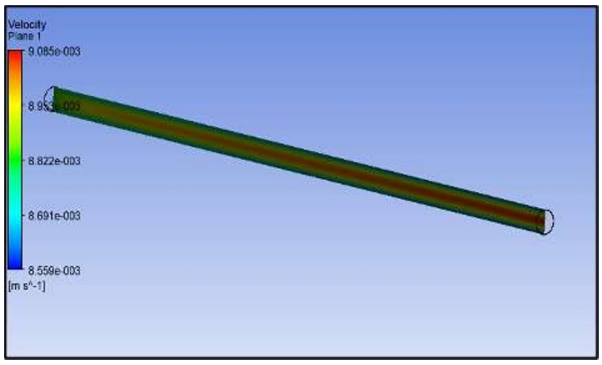

Fig. 9. Velocity plot at .005kg/s

Velocity plots in Figure 9, indicated lower velocities near the inlet i.e. 0.008m/s, increasing towards the outlet, and higher velocities at the mid-portion of the tube and reducing towards the boundary.

3.1.1 Pressure Distribution

Pressure plots in Figure 10, exhibited higher pressure at the inlet, gradually decreasing towards the exit of the absorber tube. The pressure drop was observed to decrease with an increase in mass_flow rate.

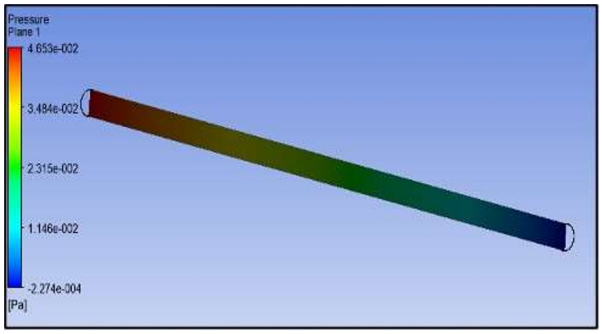

Fig. 10. Pressure plot at .005kg/s

Figure 10 shows different temperature pressure plots. The red contour shows a higher level of pressure at the inlet of magnitude 0.004 Pa, which reduces towards the exit, indicated by the light blue and dark blue contours.

3.2 Grid Independence Analysis

A grid independence evaluation was conducted, showing that increasing the number of elements resulted in a higher average temperature, indicating convergence. Table 1 below presents the results of the grid independence examination.

Table 1. Grid Independence examination

Elements (No.)	Temperature (K) Average
181256	307.71
181301	307.75
181455	307.89
181651	308.15
181668	308.15

3.3 Comparative Analysis

Comparative analysis of absorber tubes without roughness in Table 2 shows that both the Nusselt_number and pressure_drop increased with mass_flow rate. The highest values were often observed for a mass_flow rate of 0.015Kg/s. Figure 11 shows the Nusselt_number vs mass_flow rate for a tube without roughness, indicating a surge in Nusselt_number with a rise in mass_flow rate.

Table 2. Output parameters for absorber tube without roughness

Mass_flow rate (Kg/s)	Re No.	Heat_transfer Coefficient (W/m^2K)	Pressure Drop (Pa)	Nusselt No
.005	822	39.75	.045	1.77
.010	1652	94.30	.212	4.18
.015	2491	155.85	.518	6.92

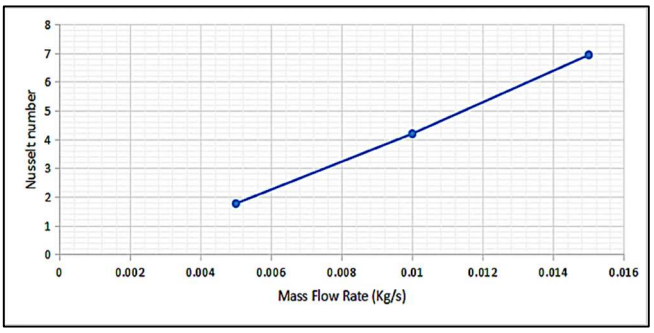

Fig. 11. Nusselt_number vs mass_flow rate for a tube without roughness

The Nusselt_number rises with higher mass_flow rates or Reynolds numbers. The peak Reynolds number corresponds to a mass_flow rate of 0.015 Kg/s. Likewise, the pressure drop rises with the mass_flow rate. The maximum pressure drops, amounting to 0.51 Pa, occur at a mass_flow rate of 0.015 Kg/s.

3.4 Parameters for absorber tube- with roughness and C-Shape

Figure 12 displays the temperature variation at a mass_flow rate of 0.005 kg/s, depicted on a lateral plane. The plot illustrates a gradual increase in temperature from the inlet (305K) to the outlet (308.5K) of the absorber tube, with higher temperatures near the wall compared to the fluid away from the wall.

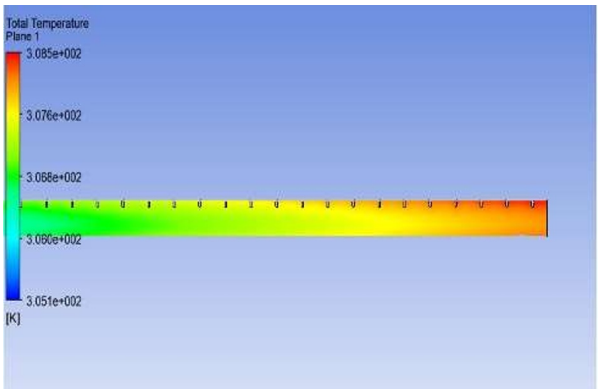

Fig. 12. Temperature plot at .005kg/s for absorber tube with roughness

In Figure 13, the velocity plot at 0.005 kg/s shows a low magnitude near the inlet (0.012 m/s), increasing as the fluid encounters the C-shaped roughness profile. The flow then intensifies at the lower and mid portions of the tube. Between the roughness elements, the air velocity significantly decreases to approximately 0.0001 m/s, as indicated by dark blue contours.

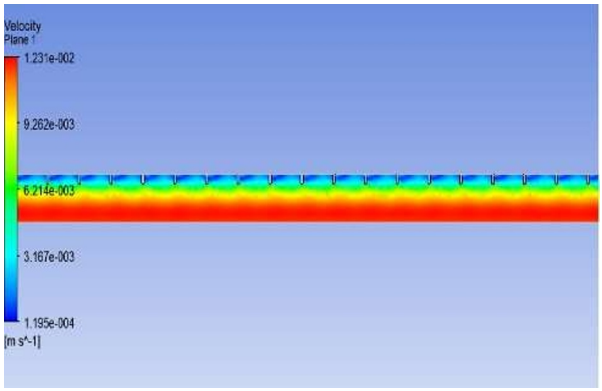

Fig. 13. Velocity plot at .005kg/s for absorber tube with roughness

Figure 14 illustrates the pressure distribution at 0.005 kg/s, with higher pressure at the inlet (0.47 Pa, shown in red contour), gradually decreasing towards the exit (light blue and dark blue contours).

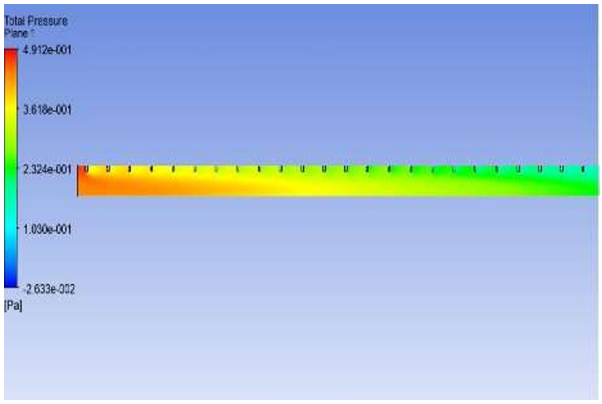

Fig. 14. Pressure plot at .005kg/s for absorber tube with roughness

Table 3 summarizes the output parameters for the absorber tube with a 5mm depth and C-shaped roughness profile, including mass_flow rate, Reynolds-number, Heat_transfer coefficient, pressure drop, and Nusselt_number.

Table 3. Output parameters for absorber tube with roughness depth 5mm and C shape

Mass_ flow rate (Kg/s)	Re number	Heat_transfer Coefficient (W/m^{2}K)	Pressure Drop (Pa)	Nusselt No
.005	851	170.85	.406	7.602
.010	1708	213.62	1.127	9.504
.015	2565	275.71	2.105	12.26

Figures 15 depict the Nusselt_number against the mass_flow rate for the tube with a C-shaped roughness profile and a depth of 5mm.

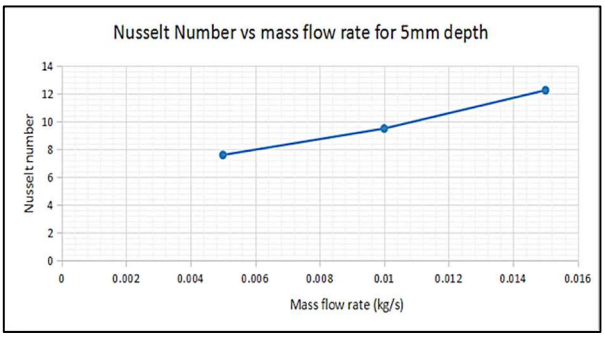

Fig. 15. Nusselt_number vs mass_flow rate for tube with c-shape roughness and depth 5mm

Similar analyses were conducted for roughness depths of 7mm and 9mm, with corresponding findings shown in Tables 4 and 5. Figures 16 and 17 associated with these tables display the Nusselt_number trends against the mass_flow rate for these respective configurations.

Table 4. Output parameters for absorber tube with roughness depth 7mm and C shape

Mass_ flow rate (Kg/s)	Re number	Heat_transferCoefficient (W/m^{2}K)	Pressure Drop (Pa)	Nusselt No.
.005	897	163.16	.613	7.258
.010	1807	246.12	1.691	10.949
.015	2717	315.88	3.157	14.052

For both the 7mm and 5mm depth artificial roughness profiles, enhancements in both Nusselt_number and pressure drop were observed with increasing mass_flow rates. The highest values for these variables were typically observed at a mass_flow rate of 0.15 kg/s.

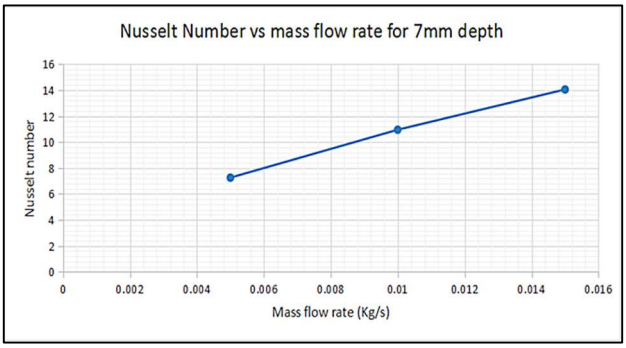

Fig. 16. Nusselt vs mass_flow rate for tube with c-shape roughness and depth 7mm.

Table 5. Output parameters for absorber tube with roughness depth 9mm and C shape

Mass_ flow rate (Kg/s)	Re number	Heat_transfer Coefficient (W/m^{2}K)	Pressure Drop (Pa)	Nusselt No.
.005	956	181.90	.88	8.093

.010	1930	272.84	2.46	12.137
.015	2905	348.52	4.62	15.504

To achieve the artificial roughness that is of the depth of 7mm and 5mm, both the Nusselt_number and pressure drop should be enhanced with mass_flow rates. The highest value of both variables is often observed for mass_flow rate (i.e. 0.15Kg/s.)

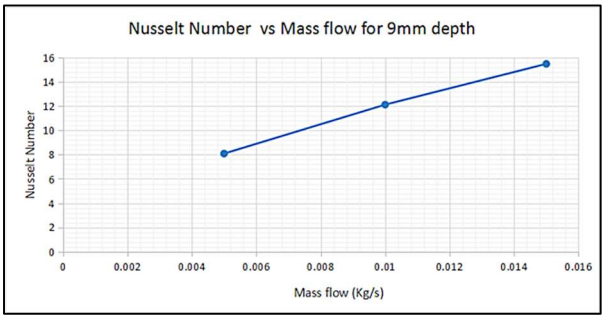

Fig. 17. Nusselt vs mass_flow rate for tube with c-shape roughness and depth 9mm

Lastly, Figure 18 presents velocity vectors at 0.005 kg/s for the C-shaped roughness profile, illustrating the disruption in flow and vortex generation between ribs due to roughness, ultimately leading to increased turbulent flow heat transfer.

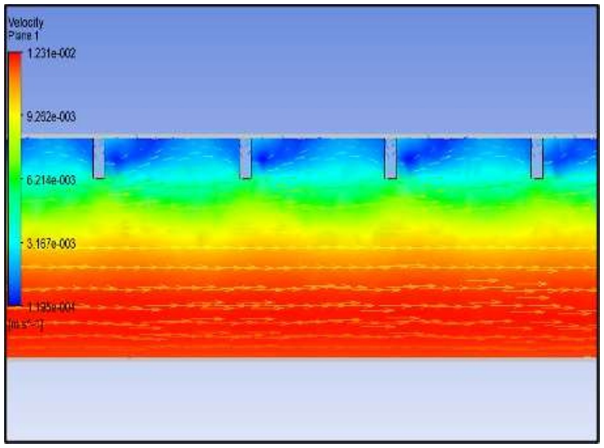

Fig. 18. Velocity vectors at .005kg/s for C-shape roughness profile

Overall, the results indicate that the incorporation of C-shape roughness profiles on absorber tubes enhances heat_transfer characteristics, with higher roughness depths showing increased Nusselt_number and pressure drop.

4 Conclusion

The results for the computational fluid dynamics analysis of the plain pipe for absorbers and for the absorbers with modified surfaces in the form of C-shaped artificial roughness at different depths (5, 7, and 9mm) showed the considerable important points about solar heat utilization and the convective heat transfer.

1. Efficiency Improvement: The smooth and artificial rough surface of the absorber tubes' modern versions was found to be more effective in the recovery of solar energy than the tube absorbers at a previous stage. Convective heat_transfer was facilitated by the use of artificial roughness at a nominal mass_flow rate (0.005Kg/s, 0.010Kg/s, 0.015Kg/s) which is shown by the Nusselt values.
2. Enhanced Heat Transfer: The C-shapes configuration with its hydraulic roughness peaked at 9mm exhibited the largest convective heat_transfer rate among the studied configurations and mass_flow rates.
3. Comparison with Smooth Tube Absorbers: The research worked out that smooth tube absorbers provided lower efficiencies than those with artificial roughness rough surface-bottom counters while offering lower heat_transfer rates.
4. Pressure Drop: Artificially rough surfaces of absorber tubes exerted higher pressure drops than those of tubes without any roughness, a direct sign of effectiveness in the heat in-circle.
5. Percentage Increase in Convective Heat Transfer: Introducing C-shaped artificial roughness caused an increment of 6.0016% in heat exchange of the convective way for the tube absorbers made by the smooth material.
6. Turbulence Model Performance: The SST model of turbulence actively strengthened the confidence in the computational results, with pressure flow patterns being predicted across the absorber tubes.

The results of this study have proven that the coating of C-shaped artificial roughness of collector tubes not only improves its effectiveness but may also be suitable for other types of solar absorbing surfaces. The identification of these research questions specifically related to roughness depth and mass_flow rate on convective heat_transfer was one of the most important success measurements. The last part of the study demonstrates its limitations to the extent. The simulations were carried out using the conditions as if in an ideal world and the real-life affecting factors, such as environmental effects, were not accounted for. Further studies might pay attention to empirical verification of the correlated results and involve more factors that can have an impact on the performance of the absorber tubes. Following such findings, it is proposed to have a look at the application of C-shaped artificial roughness on absorber tubes of the solar collector in order to enhance heat_transfer efficiency. Additional research and design improvements are required in order to obtain the best performance out of these topography features.

References

1. A. Agarwal, S. N. Mishra, and V. K. Vashishtha, Solar Tilt Measurement of Array for Building

Application and Error Analysis. Int. J. Renew. Energy Res. **2**, (2022). https://doi.org/10.20508/ijrer.v2i4.291.g6088

2. A. Agarwal, O. M. Seretse, M. T. Letsatsi, and E. Dintwa, Review of Energy Status and Associated Conservational Issues in Botswana. MATEC Web Conf. **17**, 206003 (2018). https://doi.org/10.1051/matecconf/201817206003
3. Asaad Yasseen Al-Rabeeah, Performance Analysis of a Parabolic Trough Solar Collector, Hungarian University Of Agriculture And Life Sciences, 2023
4. A. Goel and G. Manik, Solar thermal system—an insight into parabolic trough solar collector and its modeling. Renew. Energy Syst. (Elsevier, 2021), pp. 309–337. https://doi.org/10.1016/B978-0-12-820004-9.00021-8
5. Parabolic Trough Collector. SunBeam's Solar Dynamics (n.d.). https://www.solardynllc.com/parabolic-trough
6. K. Ravi Kumar and K. S. Reddy, Thermal analysis of solar parabolic trough with porous disc receiver. Appl. Energy **86**, 1804 (2009). https://doi.org/10.1016/j.apenergy.2008.11.007
7. K. S. Reddy, K. R. Kumar, and G. V. Satyanarayana, Numerical Investigation of Energy-Efficient Receiver for Solar Parabolic Trough Concentrator. Heat Transfer Eng. **29**, 961 (2008). https://doi.org/10.1080/01457630802125757
8. K. S. Reddy and G. V. Satyanarayana, Numerical Study of Porous Finned Receiver for Solar Parabolic Trough Concentrator. Eng. Appl. Comput. Fluid Mech. **2**, 172 (2008). https://doi.org/10.1080/19942060.2008.11015219
9. P. Wang, D. Y. Liu, and C. Xu, Numerical study of heat transfer enhancement in the receiver tube of direct steam generation with parabolic trough by inserting metal foams. Appl. Energy **102**, 449 (2013). https://doi.org/10.1016/j.apenergy.2012.07.026
10. P. D. Tagle-Salazar, K. D. P. Nigam, and C. I. Rivera-Solorio, Parabolic trough solar collectors: A general overview of technology, industrial applications, energy market, modeling, and standards. Green Process. Synth. **9**, 595 (2020). https://doi.org/10.1515/gps-2020-0059
11. A. Siraj, N. R. Babu, and K. S. Reddy, Static analysis of dump truck chassis frame made of composite materials. Int. J. Eng. Sci. Technol. **11**, 21 (2019). https://doi.org/10.4314/ijest.v11i2.2
12. M. R. Gomaa, R. J. Mustafa, M. Al-Dhaifallah, and H. Rezk, Cycle driven by hybrid solar collectors and a waste heat recovery system. Energy Reports **6**, 3425 (2020). https://doi.org/10.1016/j.egyr.2020.12.011
13. O. M. Seretse, A. Agarwal, M. T. Letsatsi, O. M. Moloko, and M. S. Batlhalefi, Design, Modelling and Experimental Investigation of an Economic Domestic STHW System Using T*Sol® Simulation in Botswana. In: Jayakumar V., Ranganathan S., Devika D., Sridevi S. (eds) MATEC Web of Conferences. **17**, 06004 (2018). https://doi.org/10.1051/matecconf/201817206004
14. M. Malekan, A. Khosravi, and M. El Haj Assad, Parabolic trough solar collectors. In: Design and Performance Optimization of Renewable Energy Systems (Elsevier, 2021), pp. 85–100. https://doi.org/10.1016/B978-0-12-821602-6.00007-9
15. Z. Wang, General Design of a Solar Thermal Power Plant. In: Design of Solar Thermal Power Plants (Elsevier, 2019), pp. 117–224. https://doi.org/10.1016/B978-0-12-815613-1.00003-1
16. A. Parrales, E. D. Reyes-Téllez, W. Ajbar, and J. A. Hernández, Artificial neural network applied to the renewable energy system performance. In: Artificial Neural Networks for Renewable Energy Systems and Real-World Applications (Elsevier, 2022), pp. 11–43. https://doi.org/10.1016/B978-0-12-820793-2.00006-9
17. A. K. Pandey, R. K. R., and M. Samykano, Solar energy: direct and indirect methods to harvest usable energy. In: Dye-Sensitized Solar Cells (Elsevier, 2022), pp. 1–24. https://doi.org/10.1016/B978-0-12-818206-2.00007-4
18. K. Ajay and L. Kundan, Investigation of the Parabolic Shaped Solar Collector Utilizing Nanofluid (CuO-H 2 O and SiO 2 -H 2 O) as a Working Fluid. J. Eng. 2016, 1 (2016). https://doi.org/10.1155/2016/5729576
19. M. Ilunga and A. Agarwal, A Finite-Element-Analysis-Based Feasibility Study for Optimizing Pantograph Performance Using Aluminum Metal Matrix Composites. Processes **12**, 445 (2024). https://doi.org/10.3390/pr12030445
20. O. B. Molwane, A. Agarwal, and R. Marumo, Industrial Computational Analysis of Aerodynamic Characteristics of Delta-Shaped Aircraft. In: Advances in Lightweight Materials and Structures, edited by Praveen Kumar A., T. Dirgantara, and P. V. Krishna (Springer, Singapore., 2020), pp. 761–770. https://doi.org/10.1007/978-981-15-7827-4_77
21. W. B. Musinguzi and P. Yu, Enhanced Thermal Performance of Shell and Tube Heat Exchangers Using TiO2/Water Nanofluids. J. Sustainability Energy **2**, 154 (2023). https://doi.org/10.56578/jse020305